

Organelle Segmentation Facilitated by Correlative Light Microscopy Data

Ryan Lane^{1*}, Luuk Balkenende¹, Simon van Staaldoune¹, Anouk H. G. Wolters², Ben N. G. Giepmans², Lennard Voortman³ and Jacob Hoogenboom¹

¹ Delft University of Technology, Department of Imaging Physics, Delft, The Netherlands.

² University Medical Center Groningen, Department of Biomedical Sciences of Cells and Systems, Groningen, The Netherlands.

³ Leiden University Medical Center, Department of Cell and Chemical Biology, Leiden, The Netherlands.

* Corresponding author: r.i.lane@tudelft.nl

Obtaining a more holistic understanding of cell function and morphology requires a more complete structural layout of organelles and macromolecular complexes. Currently, this level of spatial information can only be provided by nanometre-scale reconstructions of biological material from electron microscopy (EM). Deep, convolutional neural networks (CNN) can then be employed to segment these datasets for creating three-dimensional layouts of organelle distributions [1]. Training such networks, however, requires copious amounts of representative training data, which involves a great deal of human effort and time. To accumulate sufficient training data for whole-cell organelle segmentation, for instance, took over 6 months of manual labour in total [2]. An additional limitation of such approaches is that despite being an invaluable tool for investigating subcellular architecture, high-resolution EM is limited in the type of information it can provide. Various light microscopy (LM) techniques are therefore often used to supplement EM data with specific, biologically-relevant labels to aid in interpretation (correlative light and electron microscopy – CLEM).

To ascertain whether correlative LM data might be capable of facilitating organelle segmentation, we deployed an instance of ResNet-34 [3] trained on labelled images derived from CLEM datasets of cell nuclei. These datasets were obtained using integrated array tomography [4], which allows for the collection of registered EM-FM image pairs with sub-micron registration accuracy. As a naïve strategy for cheaply and automatically generating labelled images for training (segmentation masks), a threshold was applied to the correlative fluorescence images (Fig. 1C). A more sophisticated approach for generating segmentation masks was also experimented with. This method, adapted from histology applications [5], makes use of partial points annotation, in which only a single pixel is selected from a subset of the organelles in each training image. It thus serves as a supremely inexpensive annotation method while still providing some degree of human supervision. Segmentation masks are created in a two-step process. In phase one, partial points annotation is used to classify pixels as either nucleus or background, while pixels sufficiently distant from an annotation remain unlabelled. The CNN is then trained to detect nuclei that were missed during the partial points annotation. In phase two, the annotated and detected nuclei are used to partition the EM image into Voronoi cells, after which it is segmented using *k*-means clustering (Fig 1D). These processes are complimentary to one another as *k*-means clustering preserves the spatial information in the EM image while the Voronoi partition provides more accurate nuclei localization.

ResNet-34 was then trained separately on both types of segmentation masks. EM images were also manually segmented and used for training for the sake of comparison. Three regions of interest (ROI) were selected from a CLEM dataset of rat pancreas tissue and chosen for testing (Fig 2). Segmentation

performance was measured by the intersection over union (IoU). The “automated” segmentation based on thresholding the FM scored lowest (avg. IoU 48.7%; Fig. 2D). This was not unexpected as a significant amount of the labelled pixels are incorrect due to a non-uniform distribution of fluorescence in the target organelle. The “semi-automated” partial-points-based segmentation was found to perform much better (avg. IoU 84.0%; Fig 2E). Not surprisingly, however, both of these (semi-)automated mask generation methods fall short of the segmentation based on manually segmented nuclei (avg. IoU 94.7%; Fig 2D).

Although not able to outperform fully-manual-based segmentations, we have shown that registered CLEM datasets may offer a semi-automated framework for weakly supervised organelle segmentation. Such an approach may still prove useful for segmenting biological image data for certain large volume EM workflows in which a pixel-perfect segmentation may not be strictly necessary. In these cases it could serve as a valuable means of time savings at the cost of precision.

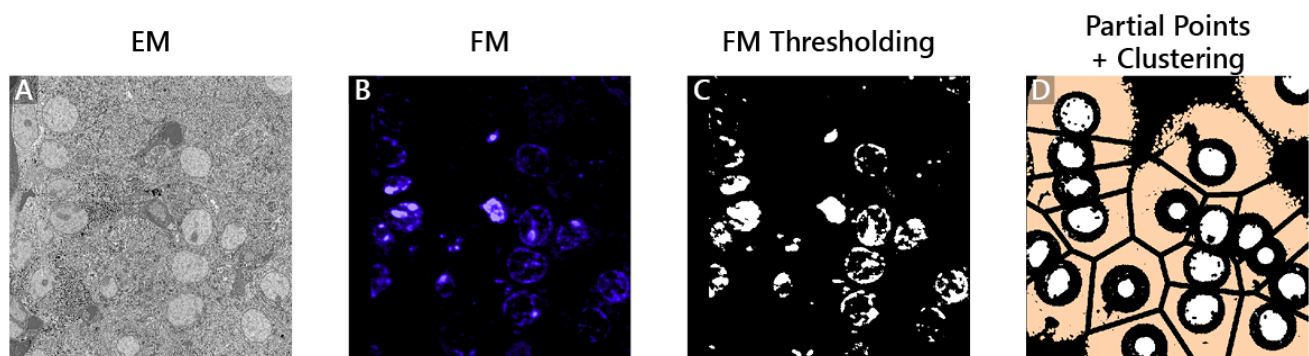


Figure 1. Different strategies for generating labelled images (segmentation masks) for training ResNet-34. (A) EM and (B) FM image pair for which a segmentation mask must be generated. (C) Mask created by thresholding the FM image (fully automated). (D) Mask created by a combination of partial points annotation and clustering algorithms (semi-automated). White: nucleus, black: background, beige: unlabelled.

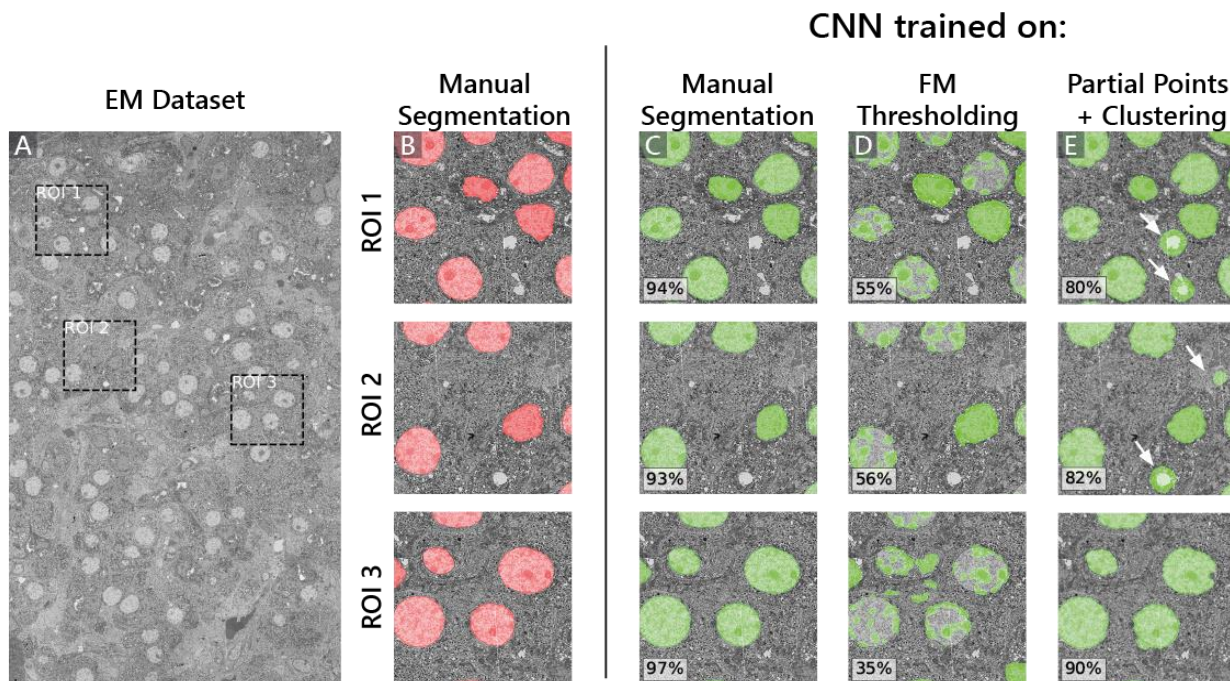


Figure 2. Cell nuclei segmentation results for a CNN trained on different types of segmentation masks. (A) EM dataset of rat pancreas tissue from which three ROI were chosen for testing segmentation performance. (B) Manual segmentation (ground truth) of cell nuclei for the three ROIs. Segmentation results of ResNet-34 trained on (C) manually segmented nuclei, (D) segmentation masks derived from thresholding correlative FM images, and (E) from partial points annotation combined with clustering algorithms.

References:

- [1] Perez, Alex J., et al. *Frontiers in neuroanatomy* **8** (2014): 126.
- [2] Heinrich, Larissa, et al. *Nature* **599.7883** (2021): 141-146.
- [3] He, Kaiming, et al. Proceedings of the IEEE conference on computer vision and pattern recognition. (2016).
- [4] Lane, Ryan, et al. *Frontiers in Molecular Biosciences* **8** (2021).
- [5] Qu, Hui, et al. *IEEE transactions on medical imaging* **39.11** (2020): 3655-3666.